IOPscience iopscience.iop.org

Home Search Collections Journals About Contact us My IOPscience

Electronic structure and optical properties of rare earth hexaborides RB_6 (R = La, Ce, Pr, Nd, Sm, Eu, Gd)

This article has been downloaded from IOPscience. Please scroll down to see the full text article.

2007 J. Phys.: Condens. Matter 19 346226

(http://iopscience.iop.org/0953-8984/19/34/346226)

View the table of contents for this issue, or go to the journal homepage for more

Download details:
IP Address: 129.252.86.83
The article was downloaded on 29/05/2010 at 04:29

Please note that terms and conditions apply.

IOP PUBLISHING JOURNAL OF PHYSICS: CONDENSED MATTER

J. Phys.: Condens. Matter **19** (2007) 346226 (10pp) doi:10.1088/0953-8984/19/34/346226

Electronic structure and optical properties of rare earth hexaborides RB_6 (R = La, Ce, Pr, Nd, Sm, Eu, Gd)

Nirpendra Singh[1], **Sapan Mohan Saini**[1], **Tashi Nautiyal**[1] **and S Auluck**[1,2]

[1] Department of Physics, Indian Institute of Technology Roorkee, Roorkee-247667, India
[2] Institute Computer Center, Indian Institute of Technology Roorkee, Roorkee-247667, India

Received 28 April 2007, in final form 10 July 2007
Published 26 July 2007
Online at stacks.iop.org/JPhysCM/19/346226

Abstract

The optical and electronic properties of the rare earth hexaborides RB_6 (R = La, Ce, Pr, Nd, Sm, Eu, Gd) are studied using the full potential linearized augmented plane wave method. To account better for the on-site f-electron correlation, we adopted the Coulomb corrected local spin density approximation (LSDA + U) to the exchange correlation functional in the calculations. Our electronic structure calculation shows the overlapping of R 5d states and B 2p states at the X symmetry point. The magnetic moment of the ferromagnetic rare earth hexaborides increases with increasing 4f occupation. The calculated reflectivity and optical conductivity spectra are in agreement with the experimental data, although the structures in the calculated optical spectra are sharper.

(Some figures in this article are in colour only in the electronic version)

1. Introduction

The divalent rare earth hexaborides (RB_6) have been studied both experimentally and theoretically. Interest in these compounds is due to the rare earth 4f electrons which play a major role in determining the electronic properties. Among the rare earth hexaborides, LaB_6 is metallic [1] and becomes superconducting at $T_C = 0.45$ K [2]. CeB_6 is a dense Kondo material and shows heavy fermion behavior [3]. SmB_6 is the first compound in which the phenomenon of mixed valence was detected by x-ray absorption [4]. EuB_6 is a ferromagnetic semiconductor with a transition temperature $T_C = 15$ K. Below T_C the electrical resistivity is drastically reduced and above T_C a very large negative magnetoresistance is observed [5]. PrB_6, NdB_6, and GdB_6 are localized 4f systems which order ferromagnetically at low temperatures [6].

The electronic structure of the rare earth hexaborides has been investigated by photoemission and inverse photoemission spectroscopy [7, 8]. Electrical resistivity measurements on EuB_6 provide evidence for a small semiconducting gap [9–11]. The transport

 © 2007 IOP Publishing Ltd Printed in the UK

properties of GdB_6 have been studied experimentally by Ali *et al* [12]. The de Haas–van Alphen (dHvA) measurements on LaB_6 [13, 14], CeB_6 [15–18], PrB_6 [18–20], and EuB_6 [21, 22] have been reported. Among these results, Arko *et al* [13] and Ishizawa *et al* [14] concluded that the Fermi surface of LaB_6 consists of a set of three equivalent, nearly spherical ellipsoids centered at the symmetry point X in the Brillouin zone. The experimental Fermi surface data of Goodrich *et al* [21] and Aronson *et al* [22] suggested that EuB_6 is a semimetal with a very low carrier concentration.

The Fermi surface of RB_6 is influenced by the 4f electrons through the f-electron contribution to the crystal potential and through the hybridization with the conduction electrons. Both mechanisms alter the electronic band structure and can change the Fermi surface topology and also the cyclotronic effective masses. Furthermore, a different magnetic structure would change the conduction-electron–f-electron hybridization, thus affecting the topology of the bands and hence the frequencies. The polarization of the Fermi surface will also be affected. Onuki *et al* [23] have measured the dHvA effect for antiferromagnetic (AFM) PrB_6 and NdB_6 and concluded that the paramagnetic (PM) Fermi surface of PrB_6 is similar to that of LaB_6, while the AFM Fermi surfaces of LaB_6, PrB_6 and NdB_6 are different. Following these observations, Behler *et al* [24] also compared the dHvA frequencies and their angular dependence of rare earth hexaborides RB_6 (R = Pr, Nd and Gd) and showed that the PM Fermi surfaces of LaB_6, PrB_6, and also of NdB_6, are very similar, while the AFM Fermi surfaces of PrB_6 and NdB_6 are very different, suggesting that the Fermi surface topology in the AFM state of the two compounds is not the same. In a recent publication [25], they have reported dHvA measurements in both PM and AFM regimes of NdB_6, and concluded that the Kondo effect is weak in NdB_6, direct exchange splitting is expected to have more responsible effect on the Fermi surface topology, and also NdB_6 can provide an essential localized f-electron precedent for understanding field induced antiferromagnetism-to-paramagnetism transitions in 4f systems. The reflectivity and the optical conductivity spectra of the rare earth hexaborides RB_6 (R = La, Ce, Pr, Nd, Sm, Eu, Gd, Tb, Dy, Ho) [26–28] and of the $Eu_{1-x}Ca_xB_6$ system [29] have been reported.

One of the earliest Fermi surface calculations of LaB_6 was performed by Hasegawa and Yanase [30], using the symmetrized non-relativistic self-consistent augmented plane wave (APW) method. Recently, the electronic structure of LaB_6 has been studied by Hossain *et al* [31] using the Cambridge Serial Total Energy Package (CASTEP) software code. Kitamura [32] have carried out the band calculations of the rare earth hexaborides RB_6 (R = La to Lu) using the modified orthogonalized plane wave (MOPW) method within the framework of the muffin tin potential approximation. A theoretical study of CeB_6 by Suvasini *et al* [33] using the fully relativistic spin polarized linear muffin tin potential (LMTO) method suggests the importance of the spin polarization and spin–orbit coupling. Self-consistent LMTO calculations have been reported for the ferromagnetic RB_6 (R = La, Ce, Pr and Nd) [34] and for the PM and AFM NdB_6 [35]. A Korringa–Kohn–Rostoker (KKR) calculation [36] for NdB_6 explains well the experimental dHvA data. LDA calculations of the band structure predict that the conduction band overlaps with the valence band at X in EuB_6 [37]. The LDA + U calculations of EuB_6 performed by Kunes *et al* [38] show that the ground state is half metallic. Antonov *et al* have performed an LSDA + U calculation of the electronic structure of SmB_6 using a fully relativistic Dirac LMTO method [39]. Calculations of the optical and magneto-optical properties [40] for EuB_6 using the full potential LMTO method indicate that spin–orbit coupling and large plasma resonance are essential to explain the experimental magneto-optical Kerr effect (MOKE).

Although the electronic structure of RB_6 has been studied by many workers, calculations of the optical properties have been performed only for SmB_6 and EuB_6 [38, 39]. It would

Table 1. Lattice constants, density of states (DOS) at the Fermi level, plasma frequency, and total magnetic moment of rare earth hexaborides.

		$N(E_F)$ (States/Ryd)			Total magnetic moment (μ_B)		
	Lattice constant (Å)	Our calculations	Previous calculations	ω_p (eV) Our calculations	Our calculations	Previous calculations	Experimental
LaB_6	4.156	11.06	11.69[c]	4.95	0.00		
CeB_6	4.141	12.01		4.90	1.03	0.941[b]	1.00[e]
PrB_6	4.121	13.04		2.56	2.77		
NdB_6	4.128	15.31		4.88	3.12		
SmB_6	4.133	20.45		2.61	5.63		
EuB_6	4.178	3.31	4.8[c]	1.32	6.99	6.98[c]	7.3[d]
GdB_6	4.112	14.30		5.14	7.88		8.01[a]

[a] Reference [28].
[b] Reference [36].
[c] Reference [40].
[d] Reference [42].
[e] Reference [52].

therefore be interesting to perform the calculations of optical properties for all the rare earth hexaborides RB_6 (R = La, Ce, Pr, Nd, Sm, Eu, Gd). The purpose of our present work is also to understand the effect of the rare earth 4f occupation on the optical properties of RB_6. In this paper, we report spin polarized full potential calculations of the electronic and optical properties of RB_6 compounds.

2. Structure and computational details

Rare earth hexaborides have the CaB_6-type crystal structure and may be viewed as a CsCl-type lattice with the cesium replaced by a rare earth ion and the chlorine by a B_6 octahedron. The experimental lattice constants [41] of the rare earth hexaborides are given in table 1. The atomic arrangement may be described in terms of the space group $Pm3m$ using its special positions: R at the (1a) site (0, 0, 0) and B at the (6f) sites $(1/2, 1/2, u)$, where u is an internal parameter, which determines the ratio between inter-octahedron and intra-octahedron B–B distances. The value of u is 0.207 for CaB_6 [41], 0.2043 for EuB_6 [42]. For the sake of simplicity, we used a fixed value for all rare earth hexaborides, as reported for EuB_6. Since the value of u changes by a small amount (a maximum of 0.003 from the value we have used) we do not expect this to make any significant changes.

As the rare earth hexaborides are ferromagnetic at low temperatures, we have performed calculations for the ferromagnetic phase. The spin polarized calculations, including spin–orbit coupling, have been performed using the FPLAPW method. Calculations are performed using the Coulomb corrected local spin density approximation (LSDA + U) method for better accounting of the correlation between the 4f electrons. The LSDA + U method is the most appropriate approximation for the rare earth compounds. The LSDA + U method explicitly includes the on-site Coulomb interaction term in the conventional Hamiltonian. There are various schemes for implementation of LSDA + U in the WIEN2K code [43]. We have used the rotationally invariant LSDA + U approximation with the double counting scheme of Anisimov [44] and collaborators. In this scheme, the exchange integral parameter J, appearing in the LSDA + U approximation, was set to its usual value for the rare earth atom of 1.0 eV, and kept fixed. The experimental value of the intra-atomic correlation energy parameter U is taken

to be 5 eV for LaB_6 and CeB_6 [45] 7.0 eV for SmB_6 [39], 9.0 eV for EuB_6 [40] and GdB_6 (as in the previous calculations), and 6.0 eV for PrB_6 and NdB_6, being intermediate between CeB_6 and EuB_6. We have chosen the exchange–correlation potential parameterized by von Barth and Hedin [46].

The atomic radii of the rare earth and boron atoms are taken to be 2.5 and 1.59 bohr, respectively, and the APW + lo basis set [47], with additional 5s and 5p local orbitals for the rare earth atom is used. The plane-wave cutoff is chosen to be $R_{mt}K_{\max} = 7$, which amounts to 631 plane waves. The numerical convergence of the total energy was better than 0.1 mRyd. To provide a reliable Brillouin zone integration, a set of 268 **k**-points in the irreducible wedge of the Brillouin zone (IBZ) was used. For the optical properties we have used 550 **k**-points in the IBZ. The convergence was also checked with a refined mesh of 1000 k-points in the IBZ with no appreciable change in energy or properties. A broadening of 0.1 eV is taken to simulate the experimental finite lifetime effects. The **k** space integration was performed using the modified tetrahedron method [48]. Since the hexaborides are cubic, there is only one component of the conductivity tensor. The interband contribution to the absorptive part of the macroscopic conductivity tensor can be obtained from the following equation:

$$\operatorname{Re}\sigma_{xx}^{\text{inter}}(\omega) = \frac{\hbar^2 e^2}{12\pi^2 m^2 \omega} \sum_{i,f} \int_{\text{BZ}} |\langle f|P_x|i\rangle|^2 \delta(E_{\text{f}}(k) - E_{\text{i}}(k) - \hbar\omega)\,\mathrm{d}k \qquad (1)$$

where $\langle f|P_\alpha|i\rangle = \mathrm{i}\hbar\langle f|\nabla_\alpha|i\rangle$ is the matrix element of the momentum operator, m and e are the mass and charge of the electron respectively, $\hbar\omega$ is the incident photon energy, $E_{\text{i}}(k)$ and $E_{\text{f}}(k)$ are the energies of the initial and final states and **k** is the wavevector inside the BZ where the transition $E_{\text{i}}(k) \rightarrow E_{\text{f}}(k)$ occurs. The intraband contribution on the diagonal part of the optical conductivity tensor is obtained from the Drude expression.

$$\sigma_{xx}^{\text{intra}} = \frac{\omega_{\text{p},\alpha}^2}{4\pi(1 - \mathrm{i}\omega\tau)}\delta_{\alpha,\beta} \qquad (2)$$

where τ is the lifetime parameter and the value of $\hbar/\tau$ is taken to be 0.1 eV.

The plasma frequency $\omega_{\text{p},\alpha}$ is calculated by

$$\omega_{\text{p},\alpha}^2 = \frac{4\pi e^2}{V} \sum_n \sum_{k\in\text{BZ}} \delta(E_{n,k} - E_{\text{F}})(\vartheta_\alpha(n,k))^2 \qquad \text{where } \vartheta_\alpha(n,k) = \frac{1}{\hbar}\frac{\partial E_{n,k}}{\partial k_\alpha}.$$

3. Results and discussion

In figures 1–3, we show the spin polarized band structures (BSs) of LaB_6, NdB_6, and GdB_6. The BS indicates a semi-metallic ground state with band overlap (R 5d and O 2p) at the X symmetry point. More importantly, the overlap of majority spin (spin up) and minority spin (spin down) is the same. The energy of the spin-up valence band is higher than that of the spin-down band. The main difference between the BSs of divalent hexaborides and LaB_6 is that the band overlapping at the X point is largest in LaB_6. Another difference among the BSs of hexaborides is that the lowest band (R p) in the BS moves away from Fermi level as one moves from LaB_6 (~ -17 eV) to GdB_6 (~ -22 eV). The bands in the valence band are more dispersive in comparison to the conduction bands.

The total density of states (DOS) along with the partial DOS for the rare earth hexaborides for spin ↑ (solid lines) and spin ↓ (dotted lines) are shown in figure 4. For the sake of simplicity, we consider the DOS for spin ↑ first. From the partial DOS, we are able to identify the angular momentum character of the states. The total DOS shows four groups of bands. The first group

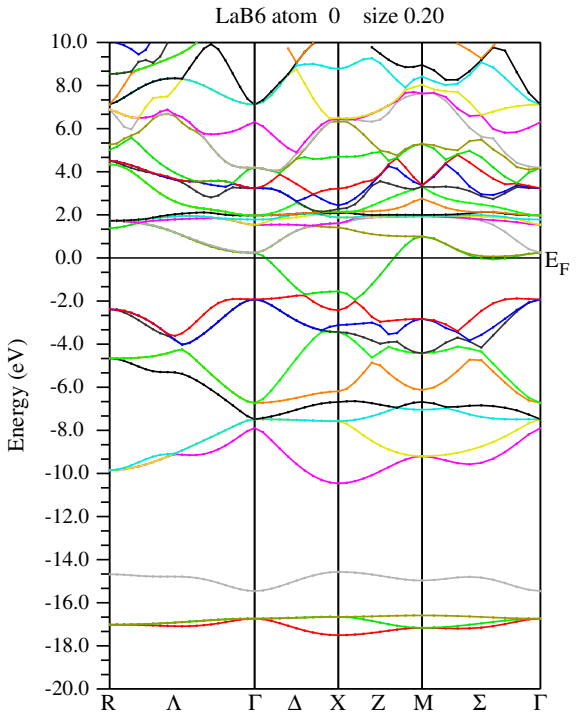

Figure 1. Spin polarized band structure of LaB_6; majority spin (solid lines) minority spin (dotted lines).

of bands consists of R p and B s states (-15 to -20 eV). The second group of bands (-10 to -2.5 eV) is characterized by B p states with some amount of R sp states. The large depth from E_F reflects the strong bonding in the B_6 octahedron cage. The 4f states present in the valence band lie at different energy levels for different hexaborides ($GdB_6 \sim 10$ eV, $NdB_6 \sim 7$ eV below E_F). This picture is fairly consistent with the x-ray photoemission spectroscopy (XPS) results [49]. The 4f band splits into two sub-bands, $4f_{5/2}$ and $4f_{7/2}$. The last group of bands (above E_F), has contributions of R 5d states, R 4f and some amount of R s states. The position of the R 5d states is different for different hexaborides. The Sm 5d band has the highest energy among the hexaborides due to the mixed valence character of SmB_6. The bottom of the conduction band and the top of valence band are formed from the hybridized R 5d states and B 2p states. The partial DOS for spin $\downarrow$ shows similar characteristics as for spin $\uparrow$, except that the 4f bands are now unoccupied. The calculated density of states at Fermi level $N(E_F)$ is lowest for EuB_6. The value of $N(E_F)$ for LaB_6 and EuB_6 is also consistent with the previous calculations [41].

The calculated total magnetic moment is given in table 1 along with previous calculations and experimental data. The spin polarized LSDA + U calculations yield zero total magnetic moment for LaB_6 because LaB_6 is nonmagnetic. We find that orbital polarization is negligible for the rare earth hexaborides. The major contribution to the total magnetic moment is from the spin polarization of the 4f electrons. The magnitude of the calculated magnetic moment is in reasonable agreement with the experimental value. Our calculations show that the value of the total magnetic moment increases as one moves from LaB_6 to GdB_6, correlating well with the increase in the occupation of 4f electrons.

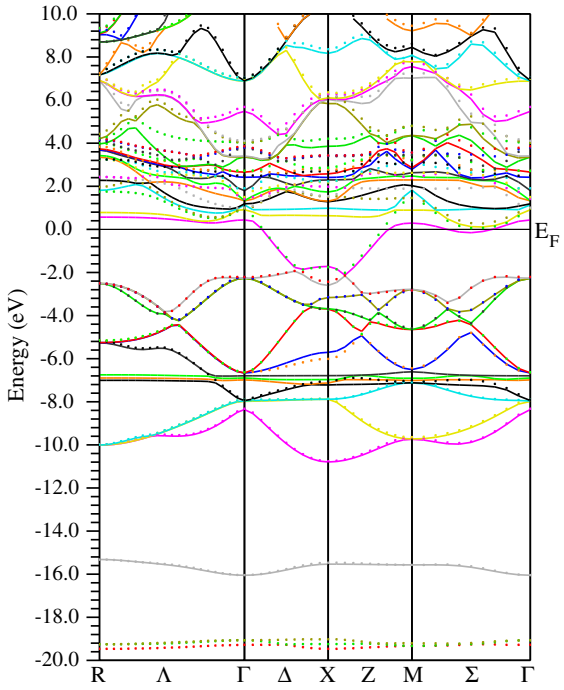

Figure 2. Spin polarized band structure of NdB_6; majority spin (solid lines) minority spin (dotted lines).

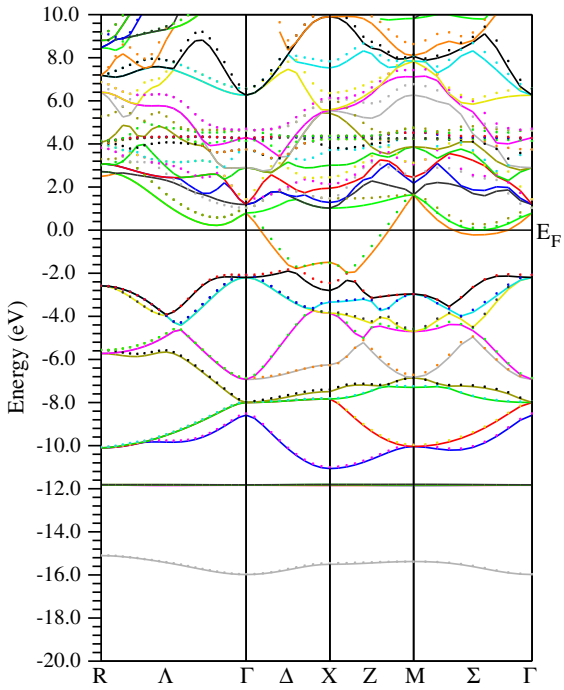

Figure 3. Spin polarized band structure of GdB_6; majority spin (solid lines) minority spin (dotted lines).

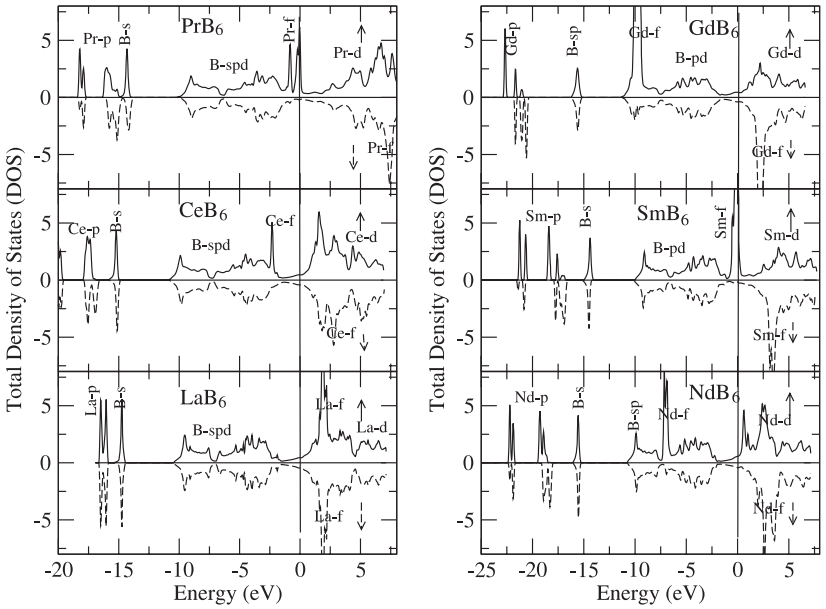

Figure 4. Calculated total density of states (DOS) for majority spin and minority spin for rare earth hexaborides.

4. Optical properties

Our calculations of the reflectivity and the optical conductivity are at zero temperature. As a result of this, the calculated spectra show many peaks and structure, which are not observed in the experimental data [26] because of lifetime broadening effects. We have used a broadening of 0.1 eV. We also include the Drude contribution (equation (2)) in the calculation of the reflectivity and the optical conductivity as the rare earth hexaborides are metallic. The calculated plasma frequency of the rare earth hexaborides is given in the table 1.

Figure 5 (left panel) depicts the calculated and the experimental [26] reflectivity spectra of the hexaborides. The experimental data show a large value of reflectivity in the low energy range. Our calculations also show this behavior. This large contribution at low energy is attributed to the Drude term. Our calculations show a dip at about 2 eV, in agreement with the experiment. In EuB_6 this dip occurs at around 0.5 eV which is the lowest among hexaborides. This may be due to the fact that EuB_6 has the smallest plasma frequency among the hexaborides. The peaks in the reflectivity spectrum are attributed to the interband transitions between B 2p states and R 5d states. The shifting of the peaks in the reflectivity spectra towards higher energy when one goes from La (unfilled) to Gd (half filled) is due to the shifting of R 5d states towards higher energy above E_F as we move from LaB_6 to GdB_6.

The calculated spectra of optical conductivity of hexaborides along with the experimental data [26] are shown in the right panel of figure 5. The calculated spectra have sharper structures as compared to the experimental data. On increasing the broadening, the calculated optical conductivity spectra agree with the experiment in terms of magnitude, but the structures are lost. The broadness of the optical conductivity spectra of EuB_6 emphasizes their low carrier density. In the interband contribution to the optical conductivity, the most prominent feature is a broad and structured peak present in the energy range 5–10 eV and 20–25 eV. This seems to signal the B 2p to R 5d transitions. The change in the character as well the relative position of the 5d

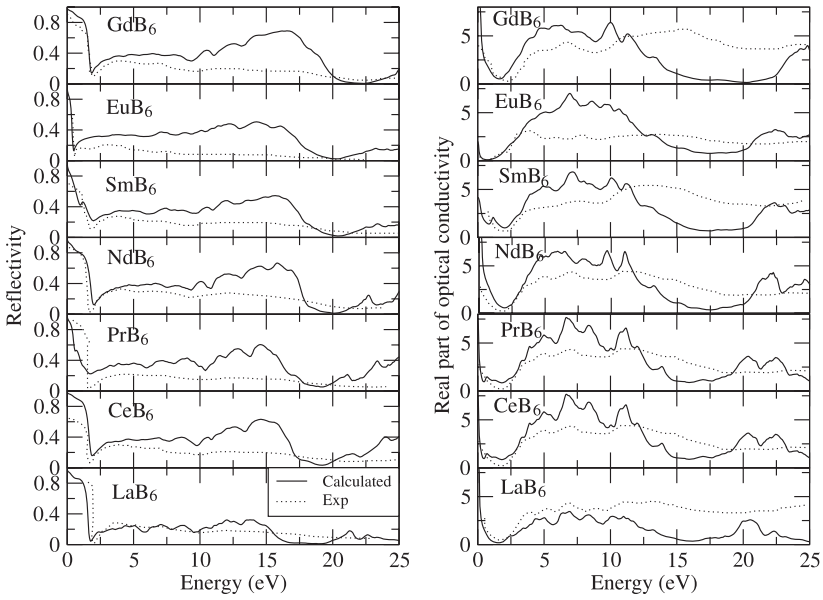

Figure 5. Calculated reflectivity (left panel) and optical conductivity (right panel) of rare earth hexaborides along with the experimental data [26].

states (as mentioned in the discussion of the DOS) should have some effect on the unoccupied conduction band. This effect is responsible for the change in the optical conductivity spectra of hexaborides in the energy range from 5 to 15 eV.

Above 5 eV the theoretically calculated optical conductivity and reflectivity spectra of rare earth hexaborides are larger in comparison with the experimental measurements. One of the possible reasons for this is a nonideal sample surface; its roughness may reduce the optical reflectivity above 5 eV. The same trend has also been reported previously, particularly for rare earth compounds [50, 51].

5. Conclusions

The spin polarized full potential calculations of the electronic and optical properties are presented for the rare earth hexaborides (RB_6, R = La, Ce, Pr, Nd, Sm, Eu, Gd) using the LSDA + U method. The BS indicates a semi-metallic ground state with band overlap (R 5d and O 2p) at the X symmetry point. More importantly, the overlap of majority spin (spin up) and minority spin (spin down) is the same. The calculated $N(E_F)$ and plasma frequency are the smallest for EuB_6 among the hexaborides. The total magnetic moment of LaB_6, CeB_6, EuB_6 and GdB_6 is in agreement with the experimental value. The value of the total magnetic moment increases from LaB_6 to GdB_6.

The calculated reflectivity and optical conductivity spectra of hexaborides have similar characteristics, in agreement with the experimental data, although the calculated structures are sharper. The interband transition between B 2p and R 5d states is responsible for the structures in the energy range 5–10 eV of the reflectivity and the optical conductivity spectra.

We have presented calculations for the rare earth hexaborides in the ferromagnetic phase, because most of the rare earth hexaborides are ferromagnetic at low temperatures. But some of them are AFM at room temperature, and therefore the calculations of rare earth hexaborides in the AFM phase are further needed.

Acknowledgments

We are grateful to the Department of Science and Technology (DST), India, for financially supporting this work through grant No. SP/S2/M-26/99. One of us (NS) would like to thank the Council of Scientific and Industrial Research (CSIR), India, for the financial support in the form of Grant No. 9/143 (436)/EMR-2002.

References

[1] Kauer E 1963 *Phys. Lett.* **7** 171
[2] Vanderberg J M, Matthias B T, Corenzwit E and Borz H 1975 *Mater. Res. Bull.* **10** 889
[3] Samwer K and Winger K 1976 *Z. Phys.* B **25** 269
Kasuya T, Takegahara K, Aoki Y, Hanzawa K, Kasaya M, Kunii S, Fujita T, Sato N, Kimura H, Komatsubara T, Furuno T and Rossat-Mignod J 1981 *Valence Fluctuations in Solids* ed L M Falokov, W Hunke and M B Maple (Amsterdam: North-Holland)
[4] Vanstein E E, Blokhin S M and Paderno Y B 1965 *Sov. Phys.—Solid State* **6** 281
[5] Guy C N, von Molnar S, Etourneau J and Fisk Z 1980 *Solid State Commun.* **33** 1055
[6] Matthias B T, Geballe T H, Andres K, Corenzwit E, Hull G W and Maita J P 1968 *Science* **159** 530
[7] Shino N, Suga S, Imada S, Saitoh Y, Yamada H, Nanba T, Kimura S and Kunii S 1995 *J. Phys. Soc. Japan* **64** 2980
[8] Suga S, Imada S, Yamada H, Saitoh Y, Nanba T and Kunii S 1995 *Phys. Rev.* B **52** 1584
[9] Johanson R W and Daane A H 1963 *J. Chem. Phys.* **38** 425
[10] Goodenough J B, Mecurio J P, Etorneau J, Naslain R and Hagenmuller P 1973 *C. R. Acad. Sci.* C **277** 1239
[11] Mecurio J P, Etorneau J, Naslain R, Hagenmuller P and Goodenough J B 1974 *J. Solid State Chem.* **9** 37
[12] Ali N and Woods S B 1984 *J. Low Temp. Phys.* **56** 575
[13] Arko A J, Crabtree G W, Karim D, Mueller F M, Windmiller L R, Ketterson J B and Fisk Z 1976 *Phys. Rev.* B **13** 5240
[14] Ishizawa Y, Nozaki H, Tanaka T and Nakajima T 1980 *J. Phys. Soc. Japan* **48** 1439
[15] Ōnuki Y, Komatsubara T, Reinders P H P and Springford M 1989 *J. Phys. Soc. Japan* **58** 3698
[16] Goto T, Suzuki T, Ohe Y, Sakatsume S, Kunii S, Fujimura T and Kasuya T 1988 *J. Phys. Soc. Japan* **57** 2885
[17] Suzuki T, Goto T, Sakatsume S, Tamaki A, Kunii S, Kasuya T and Fujimura T 1987 *Japan. J. Appl. Phys.* **26** 511
[18] van Deursen A P J, Pols R E, de Vroomen A R and Fisk Z 1985 *J. Less-Common Met.* **111** 331
[19] Ōnuki Y, Nishihara M, Sato M and Komatsubara T 1985 *J. Magn. Magn. Mater.* **52** 317
[20] Ōnuki Y, Umezawa A, Kwok W K, Crabtree G W, Nishihara M, Yamazaki T, Omi T and Komatsubara T 1989 *Phys. Rev.* B **40** 11195
[21] Goodrich R G, Harrison N, Vuillemin J J, Teklu A, Hall D W, Fisk Z, Yong D and Sarrao J L 1998 *Phys. Rev.* B **58** 14896
[22] Aroson M C, Sarrao J L, Fisk Z, Whitton M and Brandt B L 1999 *Phys. Rev.* B **59** 4720
[23] Onuki Y, Umezawa A, Kwok W K and Crabtree G W 1989 *Phys. Rev.* B **40** 11195
[24] Behler B and Winzer K 1991 *Z. Phys.* B **82** 355
[25] Goodrich R G, Harrison N and Fisk Z 2006 *Phys. Rev. Lett.* **97** 146404
[26] Kimura S, Nanba T, Kunii S and Kasuya T 1990 *J. Phys. Soc. Japan* **59** 3388
[27] Kimura S, Nanba T, Tomikawa M, Kunii S and Kasuya T 1992 *Phys. Rev.* B **46** 12196
[28] Kimura S, Nanba T, Kunii S and Kasuya T 1994 *Phys. Rev.* B **50** 1406
[29] Kim J-H, Lee Y, Homes C C, Rhyee J S, Cho B K and Oh S J 2005 *Phys. Rev.* B **71** 055105
[30] Hasegawa A and Yanase A 1977 *J. Phys. F: Met. Phys.* **7** 1245
[31] Hossain F M, Daniel Riley P and Murch G E 2005 *Phys. Rev.* B **72** 235101
[32] Kitamura M 1994 *Phys. Rev.* B **49** 1564
[33] Suvasini M B, Guo G Y, Temmerman W M and Gehring G A 1996 *J. Phys.: Condens. Matter* **8** 7105
[34] Langford H D, Temmerman W M and Gehring G A 1990 *J. Phys.: Condens. Matter* **2** 559
[35] Min B I and Jang Y R 1991 *Phys. Rev.* B **44** 13270
[36] Kubo Y, Asano S, Harima H and Yanase A 1993 *J. Phys. Soc. Japan* **62** 205
[37] Massidda S, Continenza A, Pascale T M D and Monnier R 1997 *Z. Phys.* B **102** 83
[38] Kunes J and Pickett W E 2004 *Phys. Rev.* B **69** 165111
[39] Antonov V N, Harmon B N and Yaresko A N 2002 *Phys. Rev.* B **66** 165209
[40] Ghosh D B, De M and De S K 2004 *Preprint* cond-mat/0406706

[41] Wyckoff R W G (ed) 1965 *Crystal Structures* vol 2 (Tucson, AZ: University of Arizona)
[42] Tarascon J M, Soubeyroux J L, Etourneau J, George R, Coey J M D and Massenet O 1981 *Solid State Commun.* **37** 133
[43] Blaha P, Schwarz K, Madsen G K H, Kvasnicka D and Luitz J 2001 *WIEN2K* Karlheinz Schwarz, Tech. Universitat Wien
[44] Anisimov V I, Solovyev V I, Korotin M A, Czyzyk M T and Sawatzky G A 1993 *Phys. Rev.* B **48** 16929
[45] Gschneidner K A Jr and Eyring L (ed) 1995 *Handbook on the Physics and Chemistry of Rare Earths* vol 20 (Amsterdam: North-Holland)
[46] von Barth U and Hedin L 1972 *J. Phys. C: Solid State Phys.* **5** 1629
[47] Sjöstedt E, Nordström L and Singh D J 2000 *Solid State Commun.* **114** 15
[48] Blochl P E, Jepson O and Anderson O K 1994 *Phys. Rev.* B **49** 16223
[49] Chazalviel J N, Campagna M, Wertheim G K, Schmidt P H and Yafet Y 1976 *Phys. Rev. Lett.* **37** 919
[50] Singh N, Saini S M, Nautiyal T and Auluck S 2006 *J. Appl. Phys.* **100** 083525
[51] Saini S M, Singh N, Nautiyal T and Auluck S 2006 *Solid State Commun.* **140** 125
[52] Biasini M, Fretwell H M, Dugdale S B, Alam M A, Kubo Y, Harima H and Sato N 1997 *Phys. Rev.* B **56** 10192